Viscous boundary layers at the sidewall of a convection cell

Xin-Liang Qiu and Ke-Qing Xia*
Department of Physics, The Chinese University of Hong Kong, Shatin, Hong Kong, China
(Received 25 February 1998)

Profiles of both the mean value and the standard deviation of the local fluctuating velocity were directly measured near the sidewall of a cubic convection cell using water as the working fluid. Scaling laws with the Rayleigh number Ra for various boundary layer quantities have been established over the range of Ra from 10^8–10^{10} and were found to be substantially different from those near the horizontal conducting plates where large temperature gradients exist. This in turn signifies the interplay between the temperature and the velocity fields at the horizontal plates. The length scale associated with the root-mean-square velocity is found to be analogous to the thickness of the wall layer, while the length associated with the mean velocity is analogous to the thickness of the boundary layer, in conventional wall-bounded shear flows. Our measurements also reveal that the large-scale circulation is quite uniform over a large region on the sidewall plate.
[S1063-651X(98)06807-X]

PACS number(s): 47.27.Te, 42.25.−p, 05.40.+j

I. INTRODUCTION

Several recent experiments shed new light on the nature of turbulent convection [1–4]. An important discovery in these studies is the observation of a new turbulence regime in Rayleigh-Bénard (RB) convection [1,2]. This so-called hard-turbulence state occurs when Ra is greater than 4×10^7 and is characterized by (i) a scaling relation between the Nusselt number (the dimensionless heat flux) and the Rayleigh number with a nonclassical exponent, i.e., $\mathrm{Nu}\sim\mathrm{Ra}^{2/7}$, (ii) the exponential form of the probability density function for temperature fluctuations at cell center, and (iii) the existence of a coherent circulation that spans the height of the convection cell (the so-called large-scale circulation). It has been widely recognized that the thermal and viscous boundary layers near the upper and lower surfaces of the cell play an important role in determining the heat flux and temperature statistics in the hard turbulence regime [4–6]. Recently, we have carried out direct velocity profile measurements near the bottom plates in four convection cells of cylindrical shape, with a combined range of Ra that spans from 10^6 to 10^{11} [7,8]. Our results show that the mean value and the standard deviation of the fluctuating velocity have the same scaling behavior outside the boundary region but have quite different behavior inside the boundary layer where large temperature gradient exists. The measurements also suggest that the thermal boundary layer has a stronger effect on velocity fluctuations than it does on the mean velocity [8].

To further study the interplay between the velocity and the temperature fields in the boundary layer region, we have undertaken to measure the velocity boundary layer properties near the sidewall of a convection cell. The purposes for measuring the velocity field near the sidewalls are twofold. First, the shear and the viscous layer at the insulating sidewalls and at the conducting surfaces are created essentially by the same large-scale circulation [3,7], but the steep temperature gradients (thermal boundary layers) existing at the upper and lower surfaces are absent at the sidewalls. Thus, a comparative study of the viscous boundary layer properties at the sidewall and at the conducting surface will provide insight into the interplay between the thermal and velocity fields. Secondly, measurements of the velocity field at different locations of the convection cell will provide us with a more detailed picture on the spatial structures of the large-scale circulation and the flow field in the cell. The first velocity measurements at the sidewall in the hard turbulence regime was done by Sano, Wu, and Libchaber [3] in low-temperature helium gas, which was accomplished by determining the time delay in temperature signals from a pair of bolometers. Using this method, these authors obtained the magnitude of the large-scale circulation and its scaling with Ra. By placing the bolometer pair at varying distances from the wall, they were also able to obtain a qualitative behavior for the profile of the vertical mean velocity. However, because of the nature of the technique it was not possible for them to obtain velocity profiles with sufficient precision and resolution such as the associated boundary layer quantities (shear rate, viscous layer thickness) can be extracted.

We present below results from direct measurements of the velocity profiles at the sidewall of a cubic cell with the Rayleigh number (Ra) varying from 10^8 to 10^{10} using water as the working fluid. Measurements were also made at various locations on the sidewall plate both along and perpendicular to the vertical mean flow direction.

The rest of the paper is organized as follows. In Sec. II, we give detailed descriptions of our convection cell and the method used for local velocity measurements. The experimental results are presented and analyzed in Sec. III. We summarize our findings and conclude in Sec. IV.

II. EXPERIMENT

The convection cell is a cube of dimension $L=25$ cm, the aspect ratio is thus 1. The upper and lower plates were made of copper and their surfaces were gold plated. The sidewall of the cell is formed by gluing together four transparent

*Electronic address: kxia@phy.cuhk.edu.hk

Plexiglas plates. The top and bottom plates and the sidewall were held together by stainless steel posts with Teflon spacers at the eight corners. The temperature of the upper plate was regulated by passing cold water through a cooling chamber fitted on top of the plate. To ensure uniform temperature distribution across the plate, spiral channels have been cut on the back of the top plate so that incoming and outgoing water pass each other inside the plate. The lower plate was heated uniformly at a constant rate with an imbedded film heater. The temperature difference ΔT between the two plates was measured by four thermistors imbedded inside them, two in each one. The measured relative temperature difference between two thermistors in the same plate was found to be less than 1% for both plates at all Ra, indicating that the temperature was uniform across the horizontal plates. The control parameter in the experiment is the Rayleigh number $\mathrm{Ra}=\alpha g L^3 \Delta T/\nu\kappa$, with g being the gravitational acceleration, L the height of the cell, and α, ν, and κ being, respectively the thermal expansion coefficient, the kinematic viscosity, and the thermal diffusivity of water, which was used as the convecting fluid. During our experiment, the average temperature of water in the convection cell was kept near room temperature and only the temperature difference across the cell was changed. In this way, the variation of the Prandtl number $\mathrm{Pr}=\nu/\kappa$ was kept at a minimum ($\mathrm{Pr}\simeq 7$).

The technique of *dual-beam incoherent cross-correlation spectroscopy* [9] was used to measure the mean value and the standard deviation of the local fluctuating velocity in the convection cell. Since the technique and its application to RB convection have been well documented elsewhere [9,7,8], we give only a brief description below.

The principle of the technique is simple — it involves measuring the time for a small seed particle having a velocity v in the flow field to cross two parallel laser beams in succession. The two laser beams have different colors and are separated by a known distance $\ell(\sim 0.1\ \mathrm{mm})$. Experimentally, this transit time, or delay time, is determined from the intensity cross-correlation function

$$g_c(t)=\frac{\langle I_b(t')I_g(t'+t)\rangle}{\langle I_b(t')\rangle\langle I_g(t')\rangle}=1+\beta G_c(t), \tag{1}$$

where I_b and I_g are the scattered light intensities from the two parallel beams, and $\beta(\leqslant 1)$ is an instrumental constant. In our experiment, the two beams are the blue light and the green light from an argon-ion laser operated under the multiline mode. Because there is no phase coherence between I_b and I_g, the function $g_c(t)$ is sensitive only to the scattering amplitude fluctuations produced by the seed particles moving in and out of the scattering volumes. Since the separation between the two laser beams is smaller than the typical size of thermal fluctuations, the associated refractive index fluctuations will not cause significant changes in the beam separation. With a large acceptance angle of the receiving optics, small amplitude beam wandering in the convecting fluid will also not affect the measurement of $g_c(t)$. For a turbulent flow with the probability density function (PDF) $P(v)$ of the local velocity v assumed to be of a Gaussian, $G_c(t)$ in Eq. (1) has the form [7]

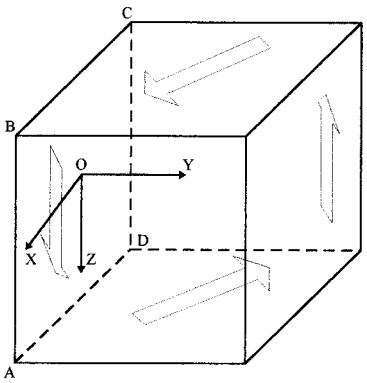

FIG. 1. Schematic drawing of the coordinate system and the large-scale circulation in the convection cell.

$$G_c(t)=\frac{e^{-(v_0 t-\ell)^2/[r_0^2+2(\sigma t)^2]}}{N\sqrt{1+2(\sigma t/r_0)^2}}, \tag{2}$$

where r_0 is the radius of the beams, N the average number of seed particles in the scattering volume, and v_0 and σ are, respectively, the mean value and the standard deviation of the fluctuating velocity.

During the experiment, the convection cell sat on top of a three-dimensional translation stage (precision 0.01 mm), so that the relative position between the laser beams and the sidewall can be easily adjusted. By fitting Eq. (2) to the measured cross-correlation function, the mean value v_0 and the standard deviation σ of the local velocity PDF $P(v)$ were obtained. It is found that the measured $G_c(t)$ at different values of Ra can all be fitted well by Eq. (2), indicating that the velocity PDF is indeed of Gaussian form as was the case in the cylindrical cell [7,8].

To determine the direction of the large-scale circulation (LSC), we employed the following method. After the convective motion was fully established, a thin stainless steel tube (diameter ~ 1 mm) with a very light string attached to its end is inserted into the convection cell; near the horizontal plate of the cell, the flow is unidirectional, so the string follows the flow and indicates its direction. Using this method, we have verified that the LSC in the cubic cell is indeed along the diagonal directions near the top and bottom plates as was observed by Zocchi *et al.* [10].

III. RESULTS AND DISCUSSION

For ease of presentation and discussion, we first define the coordinate system for the experiment. As is shown in Fig. 1, the origin of our Cartesian coordinates is at the center of one of the sidewall plates of the cell. The arrows indicate the flow direction of the LSC. In the experiment, the two parallel laser beams were shone through the cell along the x axis with their plane parallel to the sidewall plate $ABCD$. The measured velocity profile is then the vertical velocity v_z (hereafter simply v) as a function of the distance y from the sidewall.

As a characterization of the cubic cell, we show first in Fig. 2 the measured Nusselt number as a function of Ra (squares), those measured from an aspect-ratio-1 cylindrical cell (circles) are also shown here for comparison. Since the

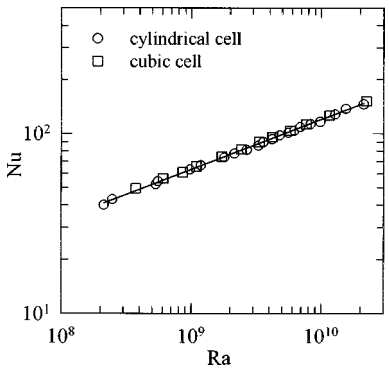

FIG. 2. Measured Nusselt number vs Rayleigh number in the cubic cell (squares), and those from an aspect-ratio-1 cylindrical cell (circles). The solid line is a power-law fit: $\mathrm{Nu}=0.19\ \mathrm{Ra}^{0.28}$.

cylindrical cell also uses water as the convecting fluid (i.e., the same Pr), the fact that the two data sets fall on top of each other suggests that the total heat transport is independent of the geometric shape of the cell as long as the aspect ratio is the same. The solid line in the figure is a power-law fit of $\mathrm{Nu}=0.19\ \mathrm{Ra}^{0.28\pm0.01}$ to the combined data set, and the scaling exponent $\beta(\simeq 0.28)$ is in excellent agreement with most experimental results from various fluid systems and cells.

Figure 3 shows a typical vertical velocity profile $v(y)$ (dots) and the corresponding standard deviation [the rms value of velocity fluctuations $\sigma=\langle(v-\langle v\rangle)^2\rangle^{1/2}$, hereafter simply referred to as rms velocity] profile $\sigma(y)$ (circles) measured at $\mathrm{Ra}=5.77\times10^9$. To allow for close examination of the boundary layer region, only the near-wall portion of the profiles are shown in Fig. 3. The complete profiles have the same general features as the ones measured near the bottom plate of a cylindrical cell [7,8]. From the measured velocity profile, three boundary layer quantities can be extracted. As is shown in Fig. 3, a linear function with zero intercept (nonslip boundary condition) can be well fitted to the initial part of $v(y)$, with the slope of the line being the shear rate γ_v. The thickness δ_v of the viscous boundary layer is defined as the distance at which the extrapolation of the linear part of $v(y)$ equals the maximum velocity v_m (which is the speed of the large scale circulation [3,7]), or

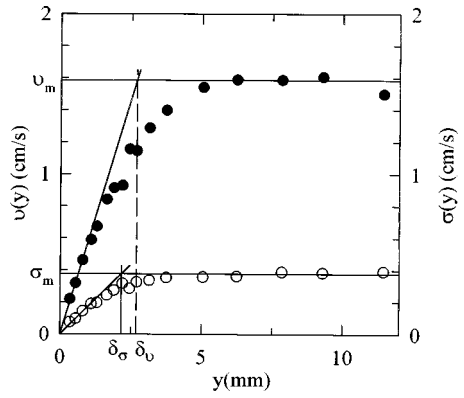

FIG. 3. The mean value v (dots) and the rms velocity σ (circles) of the fluctuating vertical velocity as functions of the distance y from the sidewall measured at $\mathrm{Ra}=5.77\times10^9$. See text for the meaning of the solid lines and other symbols.

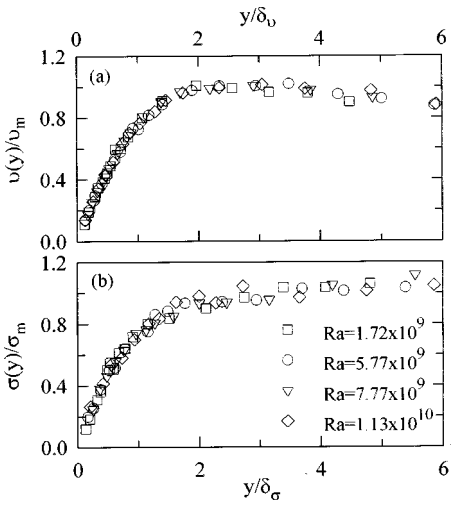

FIG. 4. Scaled mean velocity (a) and the corresponding rms velocity (b) profiles measured at four different values of Ra.

simply $\delta_v=v_m/\gamma_v$. As in Ref. [8], if we take σ as a characteristic velocity scale, then another set of viscous boundary layer quantities γ_σ, σ_m, and δ_σ can also be defined and obtained from the rms velocity profile $\sigma(y)$ as depicted in Fig. 3, where the slope for the linear part of $\sigma(y)$ is γ_σ, and $\delta_\sigma=\sigma_m/\gamma_\sigma$. It is seen from Fig. 3 that the two viscous boundary layer length scales, δ_v and δ_σ, are very close to each other, which is different from the situation near the bottom plate of the cylindrical cell [8]. We will see below that the Ra dependence of the two length scales is also different from those obtained at the conducting plates. For the present Ra ($=5.77\times10^9$), the values for the two length scales are $\delta_v=2.69$ mm and $\delta_\sigma=2.16$ mm.

The measured velocity profiles also have an invariant form, i.e., $v(y)$ for different Ra all collapse onto a single curve, once $v(y)$ is scaled by the characteristic velocity v_m and the distance y is scaled by δ_v. Figure 4(a) shows a few typical scaled profiles for four values of Ra. This invariance in functional form is also found for the profiles of the rms velocity $\sigma(y)$ when it is scaled by σ_m and y scaled by δ_σ as shown in Fig. 4(b) for the same set of Rayleigh numbers. Thus the velocity profiles near the sidewall and near the horizontal plate all have invariant forms. We also found that $v(y)$ measured at different positions along the mean flow direction (i.e., at various z) are invariant, but those measured at different x (perpendicular to the mean flow) could not be scaled to fall onto a single curve.

We now look at the positional dependence of v_m and other boundary layer quantities along the directions of x and z, i.e., streamwise and spanwise along the sidewall. Figure 5(a) shows the variation of v_m (circles) and the corresponding maximum rms velocity σ_m (dots) in the x direction at mid-height of the cell ($z=0$), Fig. 5(b) shows the shear rate γ_v (circles) and the corresponding γ_σ (dots). It is seen that none of the quantities showed significant change over a range of x extending roughly one-half of the plate ($L/2=125$ mm). In Fig. 6, we show the same quantities measured along the z direction, and no appreciable changes are seen for the maximum velocity and rms velocity in this direction either. But the shear rate seems to decay starting from the mid-height, this can be understood by the fact that the

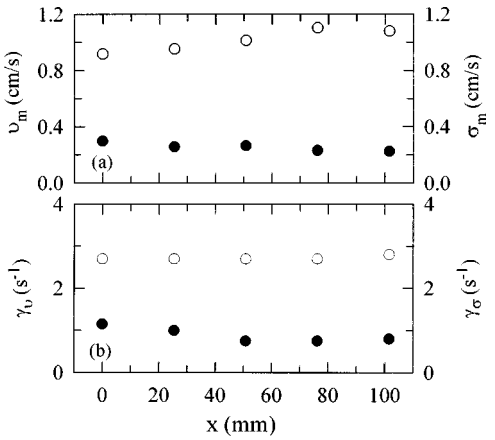

FIG. 5. Variations along the horizontal (x) direction (perpendicular to the mean flow) of the maximum mean velocity and shear, and the corresponding quantities for the standard deviation (all at $\mathrm{Ra}=2.75\times10^9$). (a) v_m (circles) and σ_m (dots); (b) γ_v (circles) and γ_σ (dots).

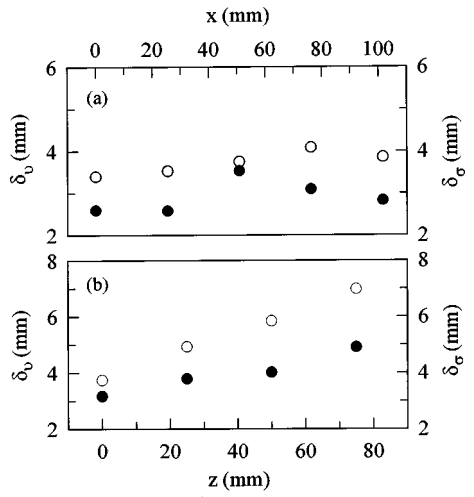

FIG. 7. Variations of the two viscous boundary layer length scales, δ_v and δ_σ, along the horizontal (a) and the vertical (b) direction, respectively.

vertical mean flow starts turning into a horizontal one as it approaches the bottom plate and therefore reduces its shear on the sidewall. The corresponding viscous boundary layer length scales $\delta_v = v_m/\gamma_v$ and $\delta_\sigma = \sigma_m/\gamma_\sigma$ along the directions of x and z reflect the behavior of the velocity and the shear rate, as shown in Figs. 7(a) and 7(b), respectively. The results shown in Figs. 5, 6, and 7 suggest that the large-scale circulation is quite uniform over a large region on the sidewall plate, and also imply that the LSC has a substantial spatial extend.

We discuss now the Rayleigh number dependence of the various quantities extracted from the mean velocity and rms velocity profiles. The results presented below are all from measurements made at $z=0$ (mid-height) and $x=50.8$ mm. Ra-dependence measurements were also made at $z=0$ and $x=76.2$ mm, and similar results were obtained. Taking the Péclet number $\mathrm{Pe}(=v_m L/\kappa)$ as the dimensionless characteristic velocity, we plot in Fig. 8 Pe as a function of Ra (circles), also plotted is the dimensionless maximum rms velocity $\sigma_m L/\kappa$ of the fluctuating velocity (squares). The upper solid line represents a power-law fit of $\mathrm{Pe}=0.36\ \mathrm{Ra}^{0.50\pm0.02}$ and the lower solid line is a power-law fit of $\sigma_m L/\kappa = 1.4\ \mathrm{Ra}^{0.38\pm0.01}$. Thus, the Péclet number has the same scaling exponent at both the sidewall and the bottom plate, whereas $\sigma_m L/\kappa$ shows a quite different behavior ($\sigma_m L/\kappa \sim \mathrm{Ra}^{0.5}$ near the horizontal plate) [8]. This difference in scaling behavior reflects the influence of the thermal boundary layer (and the associated large temperature fluctuations) existing at the horizontal conducting plates. In Fig. 9 we show the dimensionless shear rate $\gamma_v L^2/\kappa$ as a function of Ra (circles). The solid line there is a fit of $\gamma_v L^2/\kappa = (0.10\pm0.02)\mathrm{Ra}^{0.76\pm0.01}$. The squares in Fig. 9 represent the scaled gradient (or ''shear rate'') for the rms velocity, $\gamma_\sigma L^2/\kappa$ and the dashed line represents the power-law fit $\gamma_\sigma L^2/\kappa = 3.1\times10^{-2}\ \mathrm{Ra}^{0.76\pm0.02}$.

We now present and discuss the various boundary layer length scales. Figure 10 shows the scaling behavior of the nondimensional length scales $\delta_v/L = \mathrm{Pe}/(\gamma_v L^2/\kappa)$ (circles) and $\delta_\sigma/L = (\sigma_m L/\kappa)/(\gamma_\sigma L^2/\kappa)$ (squares) obtained from the mean velocity and the rms velocity profiles, respectively. It is interesting to note that the two length scales are crossed

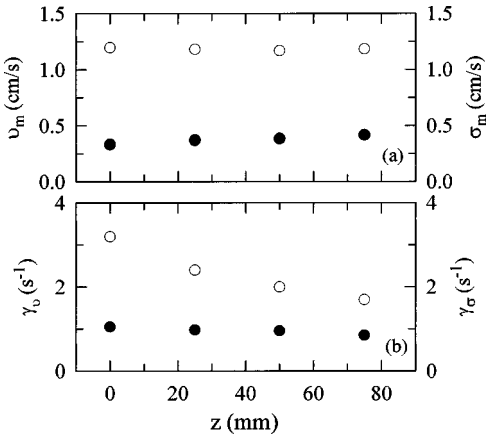

FIG. 6. Variations along the mean flow (z direction) of the maximum mean velocity and shear, and the corresponding quantities for the standard deviation (all at $\mathrm{Ra}=3.34\times10^9$). (a) v_m (circles) and σ_m (dots); (b) γ_v (circles) and γ_σ (dots).

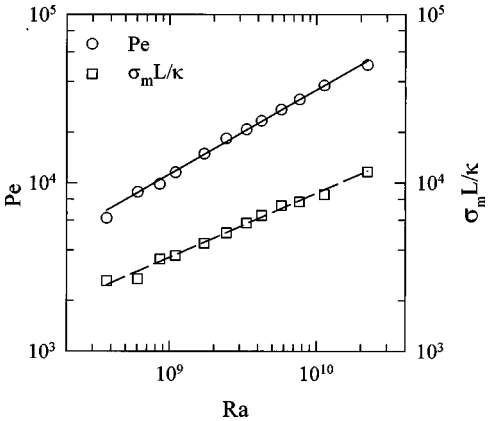

FIG. 8. Ra dependence of the Péclet number Pe (circles) and the dimensionless rms velocity $\sigma_m L/\kappa$ (squares) for the vertical mean flow near the sidewall. The solid line is power-law fit: $\mathrm{Pe}=0.36\ \mathrm{Ra}^{0.50\pm0.02}$ and the dashed line: $\sigma_m L/\kappa = 1.4\ \mathrm{Ra}^{0.38\pm0.01}$.

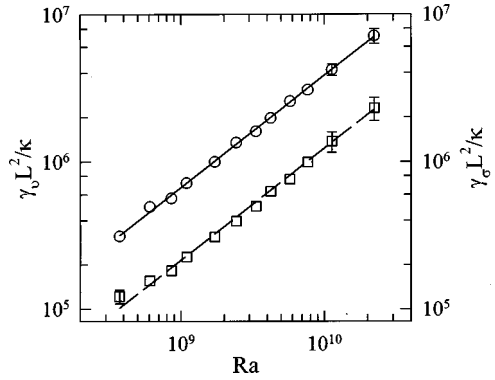

FIG. 9. The scaled shears $\gamma_v L^2/\kappa$ (circles) and $\gamma_\sigma L^2/\kappa$ (squares) vs Ra. The solid line represents power-law fit $\gamma_v L^2/\kappa = 0.1\ \mathrm{Ra}^{0.76\pm0.01}$ and the dashed line $\gamma_\sigma L^2/\kappa = 3.1\times10^{-2}\ \mathrm{Ra}^{0.76\pm0.02}$.

over at $\mathrm{Ra}\simeq10^9$, however, due to error propagation the data are more scattered than the maximum velocity and the shear rate, with which the length scales are derived. The solid line in Fig. 10 is a power-law fit $\delta_v/L = 3.6\ \mathrm{Ra}^{-(0.26\pm0.03)}$, and the dashed line $\delta_\sigma/L = 43\ \mathrm{Ra}^{-(0.38\pm0.03)}$.

We summarize in Table I the values of the scaling exponents for the various quantities measured at the sidewall, and the corresponding exponents measured at the bottom plate of the same cell [11] (which are identical to those obtained at the bottom plate of a cylindrical cell [7,8]). It is seen that except v_m, all the other quantities have different exponents at the two places. The fact that v_m has the same scaling exponent at both the sidewall and the horizontal plate is expected, as it is the speed of the large-scale circulation. However, the shears produced by the LSC at the two places are quite different, reflecting the influence of the large temperature gradient at the bottom plate. This also results in the difference in the scaling behavior of the viscous boundary layer thickness at the two places. For the maximum rms velocity and the associated length scale, the scaling behavior is quite different. This is consistent with our earlier findings at the bottom plate of the cylindrical cell that the thermal boundary layer has stronger effect on velocity fluctuations than it has on the mean velocity, and that δ_σ is the length

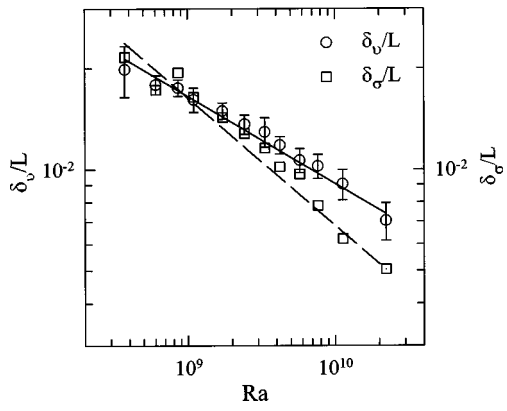

FIG. 10. The nondimensional viscous boundary layer length scales δ_v/L (circles) and δ_σ/L (squares) as functions of Ra. The solid line is a power-law fit $\delta_v/L = 3.6\ \mathrm{Ra}^{-(0.26\pm0.03)}$, and the dashed line $\delta_\sigma/L = 43\ \mathrm{Ra}^{-(0.38\pm0.03)}$.

TABLE I. Scaling exponents with the Rayleigh number for the maximum velocity v_m, the maximum rms velocity σ_m, the shear of the mean velocity γ_v, the shear of the rms velocity γ_σ, the viscous boundary layer thickness δ_v, and the length scale defined by the rms velocity δ_σ. Exponents for the measured quantities at both the sidewall and the bottom plate are listed.

Exponents of	Sidewall	Bottom plate
v_m	0.5	0.5
σ_m	0.38	0.5
γ_v	0.76	0.66
γ_σ	0.76	0.75
δ_v	−0.26	−0.16
δ_σ	−0.38	−0.25

scale over which the temperature and velocity field are coupled to each other [8]. It is also interesting to note that the scaling exponent of γ_σ is twice that for σ_m, which suggests that δ_σ is the length scale associated with the wall layer (or surface layer) in a conventional wall-bounded shear flow such as in pipes or open channels, i.e., $\gamma_\sigma \sim \sigma_m^2/\nu$ [12]. On the other hand, if δ_v is taken as the usual boundary layer thickness for a wall-bounded shear flow, then we should have $\delta_v >> \delta_\sigma$, which is clearly not the case in our system. This means there is little range here for the inertial sublayer, and the associated logarithmic profile, found in wall-bounded shear flows. In this respect, the viscous layer at the sidewall is similar to that at the horizontal conducting plate [6,7]. This means that although the viscous boundary layer at the sidewall possesses certain features the same as those for wall-bounded shear flows, it is not isolated from other parts of the convection cell and is therefore subject to the influence of the global temperature field (heat flux, plumes, etc.), which is absent in a pure shear flow.

Please note that the relation $\gamma_\sigma \sim \sigma_m^2/\nu$ does not hold at the conducting plate. This in turn indicates that, because of the strong coupling between the temperature and the velocity fields, the viscous layer at the horizontal conducting plate cannot be treated as a conventional boundary layer, which is contrary to one of the assumptions made in a model of hard turbulence [5].

IV. CONCLUSION

We have made velocity measurements near the sidewall of a cubic convection cell using water as the working fluid. Our measurements show that the large-scale circulation is quite uniform over a substantial region on the sidewall plate in the directions both along and perpendicular to the flow. The profiles for the mean velocity and the rms value of velocity fluctuations all show invariant forms for different Rayleigh number. The measurements made with varying Ra reveal that the thermal layer has a strong influence on the viscous boundary layer quantities (such as shear), while outside the boundary layer region, the velocity field is not strongly influenced. The results also confirmed our earlier findings that temperature fluctuations and velocity fluctuations are strongly coupled together. In addition, the length scale δ_σ for the rms velocity is found to be analogous to the

thickness of the wall layer (while the length δ_v for the mean velocity is analogous to the thickness of the boundary layer) in wall-bounded shear flows. The important difference is that in the convection case there is little range for the inertial sublayer associated with a conventional shear flow.

ACKNOWLEDGMENTS

We thank Y.-B. Xin and S.-L. Lui for their help with the experiment. This work was supported by the Hong Kong Research Grants Council under Grant No. CUHK 319/96P.

[1] F. Heslot, B. Castaing, and A. Libchaber, Phys. Rev. A **36**, 5870 (1987).

[2] B. Castaing, G. Gunaratne, F. Heslot, L. P. Kadanoff, A. Libchaber, S. Thomae, X.-Z. Wu, S. Zaleski, and G. Zanetti, J. Fluid Mech. **204**, 1 (1989).

[3] M. Sano, X.-Z. Wu, and A. Libchaber, Phys. Rev. A **40**, 6421 (1989).

[4] T. H. Solomon and J. P. Gollub, Phys. Rev. Lett. **64**, 2382 (1990); Phys. Rev. A **43**, 6683 (1991).

[5] B. I. Shraiman and E. D. Siggia, Phys. Rev. A **42**, 3650 (1990).

[6] A. Tilgner, A. Belmonte, and A. Libchaber, Phys. Rev. E **47**, R2253 (1993).

[7] Y.-B. Xin, K.-Q. Xia, and P. Tong, Phys. Rev. Lett. **77**, 1266 (1996).

[8] Y.-B. Xin and K.-Q. Xia, Phys. Rev. E **56**, 3010 (1997).

[9] K.-Q. Xia, Y.-B. Xin, and P. Tong, J. Opt. Soc. Am. A **12**, 1571 (1995).

[10] G. Zocchi, E. Moses, and A. Libchaber, Physica A **166**, 387 (1990).

[11] X.-L. Qiu and K.-Q. Xia (unpublished).

[12] H. Tennekes and J. L. Lumley, *A First Course in Turbulence* (MIT Press, Cambridge, 1972).